NJC

New Journal of Chemistry

An international journal of the chemical sciences

www.rsc.org/njc

Volume 32 | Number 12 | December 2008 | Pages 2053–2304

ISSN 1144-0546

RSC Publishing

CNRS CENTRE NATIONAL DE LA RECHERCHE SCIENTIFIQUE

PAPER

Bertrand Siboulet *et al.*

What can quantum chemistry tell us about Pa(v) hydration and hydrolysis?

1144-0546(2008)32:12;1-2

What can quantum chemistry tell us about Pa(v) hydration and hydrolysis?†

Bertrand Siboulet,[a] Colin J. Marsden[b] and Pierre Vitorge[c]

Received (in Montpellier, France) 15th April 2008, Accepted 3rd June 2008
First published as an Advance Article on the web 28th August 2008
DOI: 10.1039/b806407e

Published liquid–liquid extraction studies of Pa(v) were interpreted with aqueous mono-, di- and trications. B3LYP DFT is applied here to such cations surrounded by two explicit hydration layers: Linear or tetrahedral geometries are found for the Pa(v) aquo ions. PaO_2^{+} is similar to the other AnO_2^{+} cations, but has strong apical bonds, resulting from the highly negative O_{yl} charge, which decreases along the An(v) series. This explains the instability of PaO_2^{+} in water, and the differences with the heavier An(v). PaO_2^{+} diprotonates to give $Pa(OH)_2^{3+}$ and can further dihydrolyse to give T_d-$Pa(OH)_4^{+}$, which might very well be the most stable Pa(v) monocation. $PaOOH^{2+}$ is confirmed to be the Pa(v) aqueous dication invoked in the literature for pH $\leq 1.4 \pm 0.7$. PaO^{3+} is confirmed in sulfate solution, with a bond length close to 180 pm. $Pa(OH)_2^{3+}$ cannot be excluded in other conditions. The strong influence of the solvent was not fully taken into account in most previous theoretical studies that focused only on bare or partially solvated PaO_2^{+}. Toraishi *et al.* have studied hydrated Pa(v) and our work confirms this study and its qualitative interpretation. The new tetrahedral $Pa(OH)_4^{+}$ geometry that is shown here to be important opens the field to further quantum chemical studies of Pa(v) and other f-elements. As a test for the two-shell model approach for Pa(v), fluoride coordination to Pa(v) is studied and compared with published EXAFS data: an excellent fit is obtained with the well-established species PaF_7^{2-}, but most other stoichiometries tested are precluded.

Introduction

Protactinium is an actinide (An) whose chemistry is not very well known. It is probably the only natural chemical species whose aquo ions have not really been experimentally identified. Its chemistry is puzzling: Pa is not really a chemical analogue to any other An, whereas the other f-block elements are chemical analogues in aqueous solution when in the same oxidation state.

While actinides display the group oxidation state up to and including neptunium in column seven, lanthanides follow this trend only as far as cerium in group four. Praseodymium, the lanthanide situated in the same column as Pa (column five) cannot be experimentally oxidised beyond Pr(IV). Pa is thus the first actinide that shows a difference in behaviour between the two f series.

The most stable oxidation state of protactinium is five. The stable aquo ions of actinides in the +5 oxidation state (An(v)) are the AnO_2^{+} ions (An = $_{92}$U, $_{93}$Np, $_{94}$Pu and $_{95}$Am), except for An = $_{91}$Pa: PaO_2^{+} is stable only in the gas phase.[1,2]

Pa(v) has chemical analogies with Nb(v) and Ta(v), d elements of group five.[3–5] Nevertheless, theoretical calculations concluded that f-type atomic orbitals participate in Pa(v) bonding.[1] Now $_{91}$Pa is between $_{90}$Th and $_{92}$U, both of which are most stable in their group oxidation state; it is generally believed that thorium behaves as a transition metal (bonding dominated by d-type atomic orbitals), whereas the participation of f-type atomic orbitals for uranium is well established. As an example of this supposed difference in bonding behaviour, one may cite the pronounced differences in shape that characterise the ThO_2 and UO_2^{2+} isoelectronic species.[6–8] Is protactinium bonding like thorium's or like uranium's?

Actinides—and also lanthanides—are usually chemical analogues when in the same oxidation state, *i.e.* forming cations of the same charge and similar sizes. Such f-block cations can also be chemical analogues of some of d-cations with the same charge and similar size and in the same column of the Periodic Table: Y^{3+} is typically a chemical analogue of La^{3+}, Ac^{3+} and the other Ln^{3+} and An^{3+} cations, or Zr^{4+} a chemical analogue of Ce^{4+}, Th^{4+} and the other Ln^{4+} and An^{4+} cations. In most cases, however, the analogy does not hold between d and f cations. There is no chemical analogy between d and f aqueous oxo cations, again with the exception of Pa: Pa(v) displays some chemical analogies with $NbOOH^{2+}$ and $TaOOH^{2+}$.[9] It is generally believed that the f-block elements form hard cations: they behave as charged hard spheres (M^{3+} and M^{4+}) or hard linear sticks (AnO_2^{+} and AnO_2^{2+}).

[a] *Laboratoire de Conception des Architectures Moléculaires CEA, DEN, Marcoule, DRCP/SCPS, F-30207 Bagnols-sur-Cèze cedex, France*
[b] *Laboratoire de Physique Quantique, Université P. Sabatier, CNRS-UMR 5626, 118 route de Narbonne, F-31062 Toulouse cedex 4, France*
[c] *Laboratoire de Spéciation des Radionucléides et Molécules, CEA, DEN, SaclayUMR 8587DPC/SECR, F-91191 Gif-sur-Yvette cedex, France*

† Electronic supplementary information (ESI) available: Table S1: SCF energy, zero point energy and entropy of clusters used to model reactions. Table S2: Cartesian coordinates for clusters. See DOI: 10.1039/b806407e

Very few theoretical studies of Pa(v) have been published.[1,6,10–12] Most of them have focused on the PaO_2^{+} ion, which is linear at different levels of theory.[1,6] All these studies agree that the f-character of the An–O bonding increases in the ThO_2 < PaO_2^{+} < UO_2^{2+} isolelectronic series: Th–O bonds are essentially of d-character, while Pa is the first real f-element of the actinide series. The increasing f-character is associated with shortening of the An–O bond lengths, reflecting stronger bonding. Recently, Toraishi *et al.* have introduced the solvent in extensive calculations on Pa^{5+}, $PaOH^{4+}$, PaO^{3+}, $PaOOH^{2+}$ and PaO_2^{+} oxo-hydroxo Pa(v) species with one explicit hydration layer and a polarizable continuum.[3] We had shown similar structures with two hydration spheres leading to similar preliminary conclusions.[13] Toraishi *et al.* give a detailed comparison of the electronic structures of UO_2^{2+} and PaO_2^{+} that is proposed to explain the instability of PaO_2^{+} in aqueous solution. Their Mulliken population analyses indicate that the O_{yl} atomic charge is more negative in PaO_2^{+} than in UO_2^{2+}, and they propose that this explains the relative instability of PaO_2^{+}. After others,[14] they pointed out that it is hard to estimate accurate Gibbs energy changes ($\Delta_r G$) to compare with the experimental equilibrium constants for hydrolytic reactions.

Results of experimental studies are classically presented as formation constants, K (= $\exp(-\Delta_r G/RT)$), and stoichiometries of the corresponding products, typically for hydrolysis in aqueous solutions. However, for hydrolysis, only the formal number of exchanged protons can be determined, not the number of water molecules. As a consequence, such experimental results on their own cannot distinguish between aqueous species with the same charge, such as PaO_2^{+}(aq), $PaO(OH)_2^{+}$(aq) or $Pa(OH)_4^{+}$(aq) stoichiometries.[15] When the exact structure is unknown, the species can be identified through the symbol $PaH_{-y}^{(5-y)+}$ following Guillaumont's notation.[16]

Experimental results[17] can be interpreted with mono-, di- and tricationic Pa(v) species at trace concentrations in acidic aqueous solutions. Pa(v) hydrolysis experimental raw data were recently re-examined confirming the original interpretations but with increased uncertainties on the hydrolysis constants and new extrapolation to infinite dilution:[9] Pa(v) mono and dications are formed in acidic aqueous solutions in the pH range 0 to 4. The formation of a tricationic species cannot be excluded in even more acidic solutions. The successive partial—from the tricationic species as proposed by Guillaumont[18]—standard hydrolysis constants were estimated (Table 1).

These $\lg K_i^{\circ}$ values give the predominating domains of Pa(v) aqueous oxo-hydroxides (Fig. 1). They illustrate the difference with Np(v), and the other actinides(v) as they are chemical analogues of Np(v): The PaH_{-4}^{+} mono-cation has a smaller pH stability domain than the other (AnO_2^{+}) actinide(v) mono-cations (An = U, Np, Pu and Am). Furthermore, Pa(v) is much more reactive than AnO_2^{+} in the chemical conditions where the (either PaH_{-4}^{+} or AnO_2^{+}) An(v) mono-cations predominate: it is typically less soluble and easily sorbed on various materials. This indicates that the stability domain of PaH_{-4}^{+} is smaller (for Pa as compared to the other An(v)) because PaO_2^{+} is not the most stable structure of PaH_{-4}^{+}–PaO_2^{+} is hence destabilized. For this reason, we pay special attention to the actual structures of the PaH_{-4}^{+} mono-cations and their hydration.

Some authors do not rule out the existence of PaO_2^{+} in noncomplexing media,[22] but others do not mention PaO_2^{+} among the possible Pa(v) species.[5,15,23] In this paper, thanks to quantum chemistry, we try to obtain some insight into this puzzling and controversial issue. DFT methods have recently been shown to provide realistic results for the hydration of the uranyl ion when using explicit two hydration layers.[21,24,25] This method, which is very efficient for structures, has not been applied to Pa(v). We check the reliability of two-sphere model methods where possible: to the best of our knowledge, there is only one unequivocal structural determination of the nature of the Pa(v) ion in complexing aqueous solution.[17]

We begin by the application of our two-sphere models to Pa(v)-fluoride-oxo-hydroxo complexes. We show along these lines a variety of structures. We present the species in increasing charge order corresponding to decreasing stabilities with pH. This classification requires that some species are mentioned prior to their analysis. The PaH_{-4}^{+}. complexes offer a large variety: PaO_2^{+}, $PaO(OH)_2^{+}$ (two structures), $Pa(OH)_4^{+}$ (two structures). Then appear PaH_{-3}^{2+} complexes which are $PaOOH^{2+}$ or $Pa(OH)_3^{2+}$. At very low pH, we find PaH_{-2}^{3+}. complexes, namely PaO^{3+} and linear $Pa(OH)_2^{3+}$. An overview of calculated structures shows that distances are strongly correlated to the nature of the ligand, and we propose a series of values as a guideline for experiment analysis.

Methods

Most calculations were done with density functional theory (DFT) in the form of the gradient-corrected hybrid B3LYP,[26] as implemented in the Gaussian 03 program.[27] This method has recently been employed with inclusion of an explicit second hydration sphere to study the uranyl ion in aqueous solution, with pleasing success.[21,24,25] It appears that the geometrical parameters of the aquo complexes of this ion can be predicted with an accuracy of 1–2 pm. For charges, we present only the NPA[28,29] type of charge analysis rather than the traditional Mulliken analysis, since the latter is very sensitive to details of the basis sets, particularly when diffuse functions are present, as they are here. We use the NBO5.0 version modified to include 6d in the valence space, as has shown to be suited to actinides.[30]

Table 1 Pa(v) experimental hydrolysis constants, $*K_i^{\circ}$ [a]

i	1	2	3	Ref.
z	2	1	0	
$\lg *K_i^{\circ}$	$\geq -0.04 \pm 0.36$	-1.44 ± 0.71	$\ll -3.6$	[b]
			$\approx -4.95 \pm 0.2$	[c]
$\Delta_r *G_i^{\circ}$	$<0 \pm 2$	8 ± 4	$\gg 21$	[b,d]
			≈ 28	[c,d]

[a] $*K_i^{\circ} = |PaH_{-(i+2)}^{(3-i)+}||H^+|/|PaH_{-(i+1)}^{(4-i)+}|$, where $|X|$ is the activity of species X, $z = 3 - i$ is the charge of $PaH_{-(i+2)}^{(3-i)+}$ and $\Delta_r *G_i^{\circ} = -RT\ln(*K_i^{\circ})$. [b] Ref. 15 as reinterpreted in ref. 9. [c] By analogy with Nb(v).[9] [d] Calculated as $\Delta_r *G_i = -RT\ln(*K_i)$ (kJ mol^{-1}).

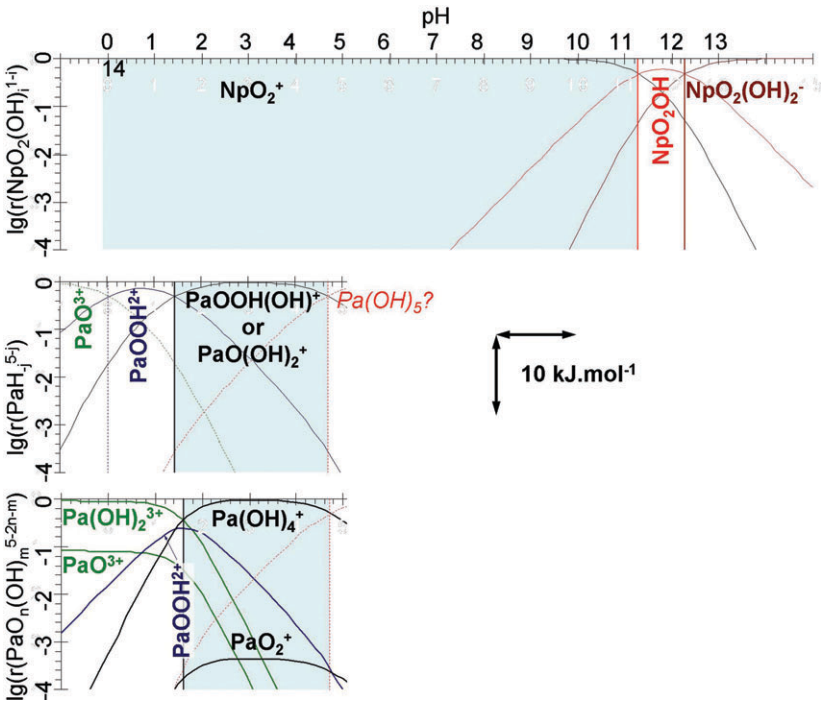

Fig. 1 Pa(v) and Np(v) aqueous species. The aqueous speciations of Np(v) and Pa(v) are calculated with equilibrium constants obtained from experiments[5,9,19–21] (top and middle figures) or from $\Delta_r G$ values estimated in the present studies from DFT calculations of two sphere Pa(v) clusters (bottom figures) at 25 °C in standard conditions. The curves are classical Sillén diagrams: $r(X_i) = [X_i]/[X]_t$ is the concentration ratio species X_i as compared to the total concentration for X = Np(v) or Pa(v). The intercept of two such curves provides the frontiers of the predominating domains: vertical lines for species of same charges (or the predominating one), since experimental solution chemistry make no difference between aqueous species of same charges. The stability of the Pa(v) neutral species is assumed to be the same as that of Nb(v).[9] Since we did not succeed to build a realistic geometrical model for the hydration of $Pa(OH)_4^+$, the predominating Pa(v) neutral species, we used the experimental stability of the mono-cationic species to plot the diagram. Dashed lines are for estimates. Note that the relative stability of the predominating trication is overestimated as compared to the experimental results, but this is within the uncertainties of the model quantum calculations. The accuracy is about of the thickness of the lines for validated data (top figure)[19] or 0.4 to 0.7 pH unit for experimental Pa data,[9] while the accuracy of our DFT model calculations is in the order of 10 kJ mol^{-1} indicated on the figure. Taking into account these uncertainties, our DFT calculations are not inconsistent with experimental results, and the predominating domain of the Pa(v) monocation is smaller than that of the Np(v) one, as a result of the destabilisation of PaO_2^+ on hydration as compared to NpO_2^+ and actually the other known AnO_2^+ cations (An is U, Np, Pu or Am (trans-protactinian)).

A "small-core" quasi-relativistic pseudopotential is used for protactinium, which treats the 60 electrons associated with the orbitals whose principal quantum number is 1–4.[31] It is established that the "semi-core" 5s, 5p and 5d electrons need to be treated explicitly.[32] The (11s, 10p, 10d, 7f) basis set associated with the pseudopotential was flexibly contracted to [8s, 7p, 7d, 4f].[32] We also used a pseudopotential for oxygen and fluorine atoms, with a "double-zeta plus polarisation plus diffuse" (DZP+) basis sets (5s, 5p, 1d) contracted to [3s, 3p, 1d] to describe the valence electrons.[33] A standard double-zeta basis set is used for hydrogen.[34] In order to check the adequacy of our DZP+ basis sets, we performed some extra calculations with all-electron triple-zeta[35] plus polarization (zeta = 0.73 on oxygen, 0.90 on fluorine) plus diffuse bases, which resulted in [6s, 4p, 1d] basis sets, and a triple-zeta plus polarization basis set for hydrogen[36] (zeta = 0.9). These larger bases produced changes in NPA charges that were typically only 0.2% for Pa, 1% for the actinyl oxygen atoms and 3% on other oxygen or fluorine atoms. Calculated distances were changed by only about 0.2% within an actinyl unit, or by no more than 1.5% for distances involving H-bonds. We conclude that the DZP+ basis sets that we used for most of this work is adequate for our purposes.

Calculations for each of $UO_2^+/UOOH^{2+}$ and $NpO_2^+/NpOOH^{2+}$ pairs were carried out with Gaussian 03. For consistency, we used similar pseudopotentials[31] and bases, the latter being flexibly contracted from (10s, 11p, 9d, 8f) to [8s, 8p, 6d, 5f] for uranium and from (11s, 11p, 9d, 8f) to [8s, 8p, 6d, 5f] for neptunium. All calculations use ultrafine integration grids and tight SCF convergence criteria.

The ADF program allows spin–orbit coupling effects to be incorporated.[37–39] Since spin–orbit coupling has an effect on energy levels, we reproduce the three $AnO_2^+/AnOOH^{2+}$ pairs of energy calculations mentioned above (An = Pa, U, Np) in the framework of ZORA (Zeroth Order Regular Approximation). In this case, we use the PW91 exchange and correlation functions, with the frozen core model and with the so-called TZ2P basis sets.

Some calculations were done at the CCSD or CCSD(T) levels of theory (Coupled Cluster with Single and Double excitations, with Triple excitations added at the perturbative level). These results include an additional g-type function on actinides, with the exponent optimized at the MP2 level (2nd-order pertubation Møller–Plesset), 0.6 for thorium, 0.7 for protactinium and 0.8 for uranium. Twenty-two electrons are

involved in the excitations. Excitations from the nine lowest-energy occupied molecular orbitals and into the corresponding virtual orbitals were excluded.

Along these lines, we examine possible structures for the (hydr)oxides present in solution. We start with gas-phase structures. We then optimise the geometries of Pa(v) aquo complexes, representing explicitly both the first and second hydration spheres, as in our previous work on the uranyl ion[25] and in recent studies.[21,24] Depending on the system, as many as 21 water molecules are treated explicitly. We did not attempt to model a third coordination sphere explicitly, since our work on the uranyl ion showed that its influence on the geometrical properties is negligible.[25]

We present a series of chemical reactions along with their estimated standard free-energy variations. In a comparison of species with different charges in a polar solvent, it is not satisfactory to ignore completely the effects of the bulk solvent on energies, since these effects can extend over a long range. We therefore report energies of the hydrated complexes obtained with a polarised continuum model (PCM), but without further geometry optimisation. Default values for the atomic radii were used, in conjunction with the van der Waals representation of the surface of the complexes. Beside these calculated values, we need two complementary data: the absolute Gibbs energy solvation of water (8.558 kJ mol^{-1} [40]) and of H^+ (1098.27 ± 25 kJ mol^{-1}.[41,42]).

The relative stabilities of Pa(v) mono- and dications in aqueous solution are published with an experimental precision on $\Delta_r G_i^\circ$ values better than ±1 kJ mol^{-1} or recently re-evaluated to ±4 kJ mol^{-1}.[9] Accuracy at this level is certainly out of reach in our two-sphere cluster-dielectric continuum approach.[24] The use of a single sphere embedded in a continuum significantly underestimates the cluster–solvent interactions, as can be observed for parameters such as the charge transfer or the vibrational frequencies,[25] but the inclusion of a second explicit sphere did not prove to be as efficient for energies as for structures.[21,43,44] Classical molecular dynamics are not impaired by the same limitations.[45] Quantum molecular dynamics should give complementary results, but very few studies exist for actinides.[46]

To help make the text easier to read, the various linear skeleton species studied will be written as C/*x*/*y*/*z*, where C represents a Pa(v) species, *x* indicates the number of water molecules in the first coordination sphere of Pa, *y* the number in the second coordination sphere, and *z* the number of additional water molecules, for example those involved in forming links to the apical atoms.

The structure of PaF_7^{2-}

To begin, we calibrate the structural accuracy of our method on an unequivocal experimental result. To our knowledge, precise structural determinations in solution exist for protactinium only in sulfuric and hydrofluoric acid media. In the latter, a structure is attributed to PaF_7^{2-} and a precise EXAFS structural determination has recently been described.[17] In HF solution, PaF_7^{2-} is reported to be dominant for HF concentrations ranging from 10^{-3} to 4 M.[47] EXAFS results indicate a single bond distance, Pa–F = 216(2) pm. Now EXAFS does not allow coordination numbers to be determined with precision, and it cannot readily distinguish between atoms that are neighbours in the Periodic Table, such as O and F. We show that the fit of quantum chemistry structures to the EXAFS data allows us to rule out most possible complexes.

We first consider all the complexes whose charge is −2 that include Pa, O and F in one-sphere models,[13] eliminating the most inconsistent with experiment. We then refine the remaining structures with two-sphere models.

Do the EXAFS results preclude the presence of water molecules in the Pa first-coordination sphere?[17] The experimental Pa–ligand distance is 216 pm. To our knowledge, all experimental results indicate a water–actinide or –lanthanide distance much closer to 240 pm than to this value, regardless of the oxidation state or total complex charge. For the smallest lanthanide(III), lutetium, a distance of 234 pm has been observed.[48] On the other hand, 216 pm is a typical well-established value for an actinide–fluoride or actinide–hydroxide distance, as exemplified in reference.[49] We show typical values in Table 6. The presence of water in the vicinity of Pa at the distance of 216 pm is thus precluded. Computational results for other hypothetical fluoride-containing structures whose charge is −2 are presented in Table 2, Fig. 2 and 3. Structures S2-1 and S2-2 contain four fluoride ions in the equatorial plane; the axial unit is PaOOH for S2-1 but PaOF for S2-2. Neither of these structures is compatible with all the experimental data. The average distance agrees satisfactorily with experiment in both cases. However, the EXAFS experiment shows only a single, narrow peak for first-sphere distances to Pa (twice the mean average displacement is 14 pm, and a substantial fraction of this width is due to vibrational motion), whereas the maximal computed differences in Pa–X distances with X = O or F, Δ-Max, are 34.1 and 33.5 pm for S2-1 and S2-2, respectively. The incompatibility results from the PaO bond which is too short.

Structure S2-3 contains a $Pa(OH)_2^{3+}$ linear unit and five equatorial ligands, S2-4 contains an axial PaFOH unit and five equatorial fluoride ions, while S2-5 contains only fluoride (PaF_7^{2-}). The computed distribution of Pa–X distances (average and Δ-Max) is in fair agreement with the EXAFS experiment for these three species.

In an attempt to discriminate between them, we add a layer of water molecules to mimic the solvent. This can produce significant changes to the first-sphere structure. For example, the uranyl–water distance is reduced by 6 pm upon inclusion of the medium, either explicitly or *via* PCM.[25] It is important to realise that the solvent influence cannot be anticipated even in the simplest cases: for PaF_n^{5-n}, links with external molecules lengthen the first-sphere bonds, but charge transfer to solvent molecules reduces repulsion between the negative ligands, and thus shortens the first-sphere bonds. We propose two-sphere complexes that are representative of the solvent, but we do not claim that they represent the solvated complexes exactly. In S2-6 (S2-3 hydrated by 16 H_2O molecules), the influence of the solvent changes the OH^- and F^- coordination distances in opposite directions. The difference of solvent effects on those two ligands has been studied for complexes of the uranyl ion.[50] In S2-6, the maximal difference is now substantially larger than the width of the experimental single

Table 2 Bond distances (pm) for Pa complexes containing oxygen and fluoride, charge −2, that exclude water[a]

	Exp.[12]	S2-1 One-sphere	S2-2	S2-3	S2-4	S2-5	S2-6 Two-sphere	S2-7	S2-8
Structure		C_s	C_{4v}	D_{5h}	C_s	C_1	C_s	C_1	C_2
Stoichiometry	PaF_7^{2-}	$PaOOH/4F^{2-}$	$PaOF/4F^{2-}$	$Pa(OH)_2/5F^{2-}$	$PaFOH/5F^{2-}$	PaF_7^{2-}	$Pa(OH)_2^{3+}/16H_2O$	$PaF_6OH^{2-}/14H_2O$	$PaF_7^{2-}/12H_2O$
Average	216	218.4	217.6	220.5	220.3	218.9	221.7	219.4	218.0
Minimal	—	O/190.5	O/190.3	O/218.0	F/218.5	F/218.0	O/203.4	O/207.2	F/216.2
Maximal	—	F/224.6	F/223.8	F/221.5038	O/223.7	F/220.0	F/230.4	F/225.3	F/222.5
Δ-Max (2σ)	14	34.1	33.5	2.5	5.2	2.0	27.0	18.1	6.3

[a] The calculated structures with a total charge of −2 are compared with experiment. All distances in pm. The minimal and maximal distances refer to Pa–O or Pa–F distances, the atom type being indicated in each case. The average distances include all F and O atoms. 2σ is twice the experimental mean average displacement. All the structures are shown in Fig. 2 and 3. All structures are drawn with MOLEKEL.[51,52]

distance peak, and the seven ligand to Pa average distance is overestimated. The misfit with experiment is significant. In S2-7 (S2-4 hydrated by 14 H_2O molecules), the fit to experiment is acceptable. The PaO_{OH} distance is maximal in S2-4 but minimal in S2-7: the bond-length order with fluoride is reversed. It can be argued that Δ-Max in S2-7 would be changed by thermal agitation, so a dynamic study would be appropriate, but that is beyond the scope of this study.

In S2-8, each fluoride is H-bonded to two water molecules (Fig. 2). The modelled average distance differs from the EXAFS value by only 0.8%, and the spread of Pa–F distances of only 6 pm is quite consistent with the EXAFS data. This

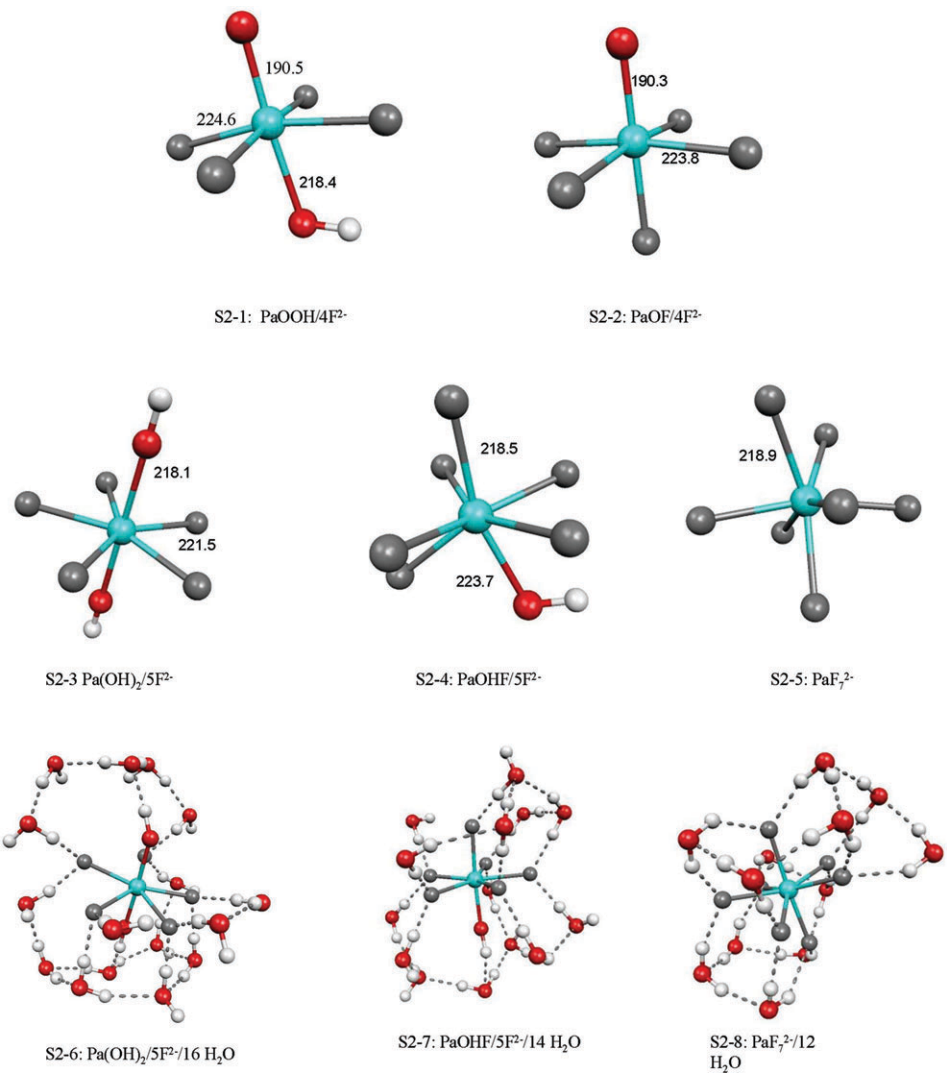

Fig. 2 −2 Charged Pa(v)-fluoride-oxo-hydroxo complexes, one and two layer clusters. The best fit is for PaF_7^{2-}. Hydration has small impact on structure. Distances in pm.

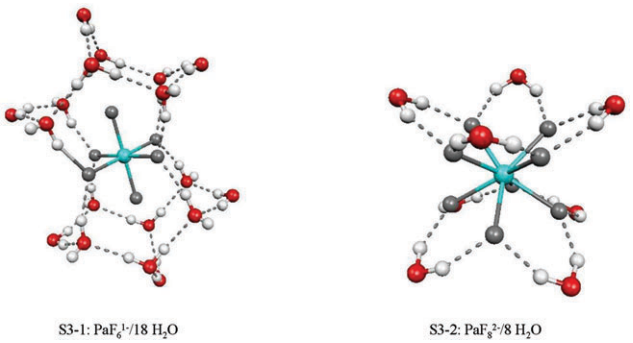

Fig. 3 The PaF_n^{5-n} Pa(v)-fluoride series, $n = 7$, is definitely the only acceptable fit with experiment. Hydration has small impact on distances.

complex, although only representative of the solvent, enables us to infer that the solvent changes the distances, but only by about 1 pm on the average. This very small distance change indicates that it is not necessary to compute other two-sphere structures. The symmetry of S2-8 is higher than that of S2-5. This is an attempt to increase Δ-Max, since the experimental σ value is small. In S2-8, C_2 symmetry creates four distinct types of fluoride ligands, and still Δ-Max is within experimental limits. In conclusion, S2-8 is a better fit to experiment than S2-7, but the difference is not decisive. S2-6 can be discarded.

We now consider the PaF_n^{5-n} series in Table 3 and Fig. 3. The Shannon ionic radii fit to within 0.5%. With S2-5 (PaF_7^{2-}), we reproduce precisely the published results.[10] In the PaF_n^{5-n} series, PaF_7^{2-} is definitely the best fit to experiment.

We underline that in this case, if the PaF_7^{-2} stoichiometry were not well-established, as is the case for Pa-chloride complexes,[17] the comparison of theoretical and experimental distances would be a powerful tool for speciation.

The structure of PaO_2^+

A tentative structure for PaO_2^+

We now consider the geometry and electronic structure of PaO_2^+ in the gas phase. The existence of this ion has been assessed in vacuum, both experimentally[2] and theoretically.[1,6] This ion is isoelectronic to the uranyl ion; both are linear and have triple bonds. When a first hydration layer is added to PaO_2^+, assuming D_{5h} symmetry as for the analogous $[UO_2(H_2O)_5]^{2+}$ species, the resulting structure is unexceptional, and is also supported by Toraishi *et al.*[3] However, addition of second hydration layer produces a structure which cannot reasonably be described as PaO_2^+/5/10: on geometrical relaxation, the water molecules in the second layer adopt a position which is intermediate between an apical hydrogen bond and one to the water molecules in the first layer, giving a structure which is not geometrically "close-packed". In particular, the structure does not show H-bonds between first and second layer molecules as they usually appear in this type of calculation: H···O–H linear and an H–O distance close to 190 pm. This geometrical instability can clearly be traced to the very high negative charge on the yl oxygen atoms in PaO_2^+/5/10/6 (−0.961 *e*, compared to −0.968 *e* in an isolated water molecule, with NPA analysis). Whereas the addition of apical hydrogen bonds to the UO_2^{2+}/5/10 species is merely a useful refinement to the model, their addition is necessary for the PaO_2^+/5/10 case if a geometrically realistic structure, such as S4-6 in Fig. 4, is to be found.

Table 3 PaF_n^{5-n} series: average Pa–F distances[a] for one- and two-sphere structures

PaF_n^{5-n}	PaF_6^-	PaF_7^{2-}	PaF_8^{3-}
No solvation (one sphere)	[b]	S2-5	[b]
Point group	O_h	C_1	D_{4d}
Average distance	212.0	218.9	225.9
With solvation (two sphere)	S3-1	S2-8	S3-2
Point group	D_{4h}	C_2	D_{4d}
Average distance	212.0	218.0	224.2
Shannon ionic radii	211	—	224

[a] Distances in pm. Shannon ionic radii are extracted from ref. 17 [b] Structure not shown.

PaO_2^+ compared with its closest isoelectronic compounds, ThO_2 and UO_2^{2+}

As stated earlier, we are aware of very few theoretical studies of PaO_2^+. Dyall analysed the three isoelectronic systems ThO_2, PaO_2^+ and UO_2^{2+},[6] and discussed the factors that determine their geometries: ThO_2 is bent, with a bond angle of about 120°, but PaO_2^+ and UO_2^{2+} are both linear. Dyall showed that the key feature is the relative energies of the 5f and 6d orbitals.[6] 5f lies above 6d for Th, but slightly below for Pa and substantially below for U. Straka, Dyall and co-workers have also studied PaO_2^+ with various theoretical methods and with several basis sets. At the correlated level, they report bond lengths that are very close to our DFT value.[1]

The ground-state configurations of the atoms (Th $6d^27s^2$, Pa $5f^16d^27s^2$ and U $5f^36d^17s^2$) imply that the importance of the 5f functions in the bonding of these systems grows as the atomic number increases. In an attempt to quantify this change, we have studied ThO_2, PaO_2^+ and UO_2^{2+} both with and without f-type functions in the basis set and report the B3LYP results in Table 4. We present the optimised geometries for both basis sets, the energy lowering obtained when f-type functions are added at the geometry optimised without them and the additional energy lowering obtained on geometry optimisation when the f-type functions are present. All three systems are strongly bent if f-type functions are excluded, and both the geometrical and energetic changes that result from the addition of f-type functions increase strongly from ThO_2 through PaO_2^+ to UO_2^{2+}. We conclude that the importance of f-type functions is moderate for ThO_2, but large and very large for PaO_2^+ and UO_2^{2+}, respectively.

PaO_2^+ compared with its AnO_2^+ successors

Since PaO_2^+ shows electronic similarities with higher linear actinides, we compare it to the latter in the +5 oxidation state. As indicated previously, the charge on the oxygen atoms in PaO_2^+ (O_{yl}) is highly negative. This is a first hint that PaO_2^+

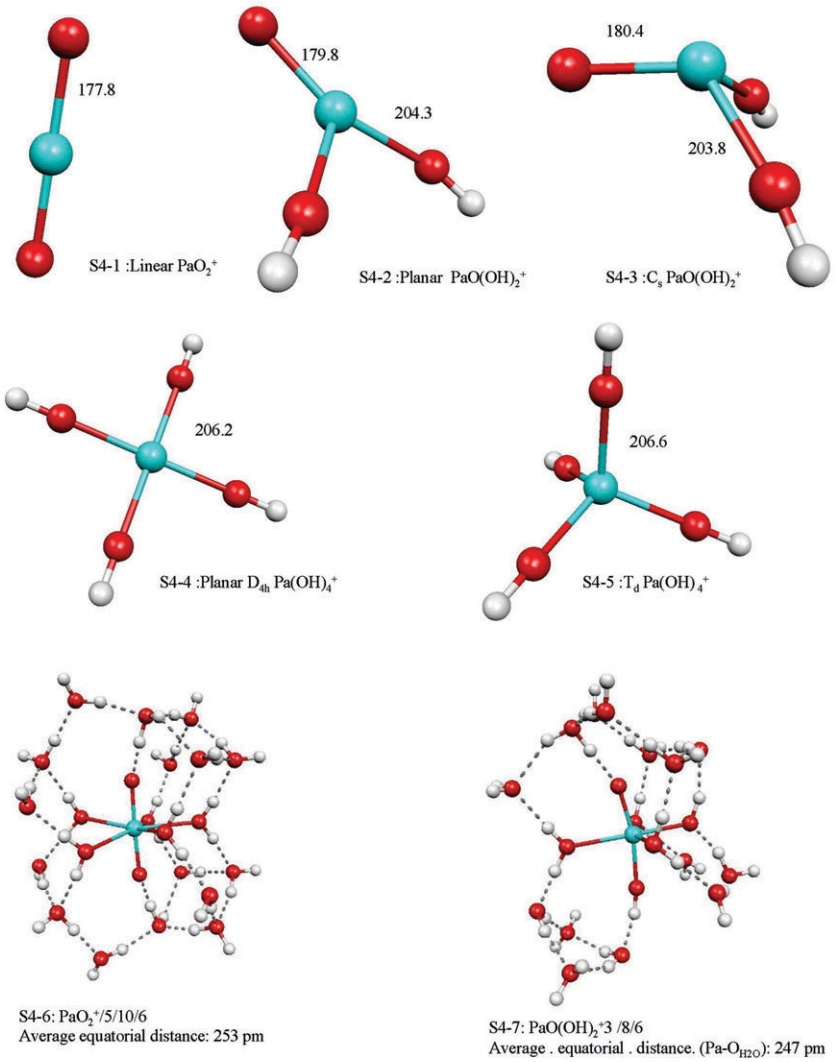

Fig. 4 Protactinium(v) monocationic species in gas phase (S4-1 to 5) and two-layer hydrated (S4-5 and 7). Distances in pm.

is unstable in solution. Since NpO_2^+ is stable up to pH = 11.3,[19,20] it is necessary to confirm this first indication by comparing charges in the series Pa–U–Np(v). The comparison implies that spin–orbit coupling is taken into account, since it can affect orbital ordering in open-shell complexes, as well as multiplet effects when 2 or more electrons are unpaired.[53] The electronic structures were determined with ADF, using the PW91 exchange and correlation functionals, both with scalar and spin–orbit coupling. The use of the intermediate Hamiltonian Fock-space coupled-cluster method confirms that fϕ is occupied in UO_2^+ [54] and that fδ and fϕ are occupied in NpO_2^+.[55] The NPA charges result from the corresponding electronic structure calculation with the Gaussian program at the B3LYP DFT level. The results in Table 5 show that the charge on O changes quite strongly in this series, with NpO_2^+ being the least polarised. PaO_2^+ is a closed-shell system: higher AnO_2^+ have extra non-bonding electrons which belong to the An and reduce the polarisation.

Table 4 Influence of f orbitals on the structures and energies of AnO_2^{+x}

	ThO_2			PaO_2^+			UO_2^{2+}		
AnO_2	d^a	θ^b	ΔE^c	d^a	θ^b	ΔE^c	d^a	θ^b	ΔE^c
No f functions	202.1	102.6		193.9	99.4		188.3	97.7	
With f functions[d]			318			714			1523
Optimization[e]	190.4	118.7	58	177.7	180	164	170.5	180	237
All-electron DHF[8]	189.8	120.4		174.2	180		165.0	180	

[a] Distances (d) in pm. [b] Angles (θ) in degrees. [c] Energy change in kJ mol^{-1}. [d] ΔE on this row is the energy lowering obtained when f-type functions are added (single-point energy shift) at the geometry optimized without them (previous line). [e] ΔE on this row is the additional energy lowering (extra energy shift over and above the single-point one) obtained on geometry optimization when the f-type functions are present (previous line).

The substantially more negative charge on the oxygen atoms in PaO_2^+ has two important consequences: the formation of very short hydrogen bonds to the yl oxygens in aqueous solution, and a highly energetically favourable mono- or diprotonation (see the following sections). Fig. 4 shows the hydrated PaO_2^+ complex we calculated (structure S4-6). The distance between O_{PaO} and the apical H_{H_2O} is close to 155 pm. This H-bond length distance is unusually short, indicating a

Table 5 Structures and charges on the early AnO_2^+ series (NPA charges, in electrons; distances in pm)

AnO_2^+	PaO_2^+	UO_2^+	NpO_2^+
Electronic state	$^1\Sigma_g^+$	$^2\Phi_u$	^3H_g
O-NPA charge:			
Bare AnO_2^+	−0.74	−0.66	−0.59
Two-sphere + apical link	−0.96	—	—
Distances:			
O_{yl}-An, calc.	189	—	—
An–O_{H_2O}, calc. (av.)	253	—	—
O_{yl}–An, exp.[56]	184[a]	183[a]	182[56]
An–O_{H_2O}, exp.[56]	253[a]	251[a]	249[56]
O_{yl}–An, exp.[41]	187[b]	185[b]	183[41]
An–O_{H_2O}, exp.[41]	256[b]	253[b]	250[41]
Proton exchange electronic energy between Pa and U or Np:[c]			
Scalar relativistic	0	−41	−67
Spin–orbit coupling	0	−40	−66

[a] Extrapolated from the experimental PuO_2^+ structure, Pu–O_{yl} being equal to 181 pm and Pu–O_{H_2O} being equal to 247 pm.[56] [b] Extrapolated from the experimental PuO_2^+ structure, Pu–O_{yl} being equal to 181 pm and Pu–O_{H_2O} being equal to 247 pm.[57] [c] Calculations are performed with ADF and the PW91 exchange and correlation functionals. See text for reactions (8) and (9).

strong apical link, whereas for hydrated UO_2^{2+}, we found a distance between O_{yl} and the apical H_{H_2O} of 192 pm,[25] which is also a typical value for a water–water H-bond.

As far as we are aware, there is no experimental structural information for PaO_2^+, either in the gas phase or in aqueous solution. However, such information does exist for Pu(v) and Np(v) from different sources. Since they follow PaO_2^+ in the actinide series, the actinide contraction allows us to extrapolate tentatively to protactinium. In Table 5, for PaO_2^+, our calculated axial distance exceeds the extrapolated values by only 1 or 2%. This small overestimation of the actinyl bond length is comparable to the results we have previously obtained for uranyl with similar methods.[25] The average equatorial distance is underestimated by 0 or 1%.

Conclusion for PaO_2^+

We have calculated a two-sphere hydrated structure for PaO_2^+. Calculated data are consistent with those obtained experimentally for higher actinides(v). The short apical H-bonded link and the highly negative charge on O_{yl} for the solvated complex indicate that solvation makes the PaO_2^+ species unstable. Toraishi *et al*. also recently pointed out that the highly negative charge of O can explain the instability of PaO_2^+ in aqueous solutions.[3] Adding two solvation layers, apical H-bonds are formed, and one or two protons are easily added on the oxygens, as will be established later.

Other PaH_{-4}^+ species

A variety of structures can be constructed from PaO_2^+ by addition of one or two water molecules. All the structures are plotted in Fig. 4. Among these PaH_{-4}^+ species, the activity ratios are constant in liquid water, and in particular are independent of pH. This is noteworthy, considering the extent of the pH domain of PaH_{-4}^+: $(1.44 \pm 0.71) \leq pH \ll (4.95 \pm 0.2)$ (see Introduction)

The structures of $PaO(OH)_2^+$

Addition of a single water molecule to PaO_2^+ can result in $PaO(OH)_2^+$, which we first consider in vacuum. Since $PaOOH^{2+}$ is stable (see below), we first build an planar constrained geometry by addition of an hydroxide in the equatorial plane (structure 4-2, Fig. 4). The resulting planar structure is unstable. Its NBO analysis results in seven bonds, each hydroxide being doubly bounded to Pa. The two hydroxides are not exactly equivalent in this constrained structure, since we observe an axial one and an equatorial one, but the two hydroxide to Pa distances are very similar.

Upon relaxation, we find the S4-3 (Fig. 4) stable quasi-C_3 pyramidal C_s structure, PaO lying in the symmetry plane, with O–Pa–OH angles equal to 114°, and a dihedral O–Pa–O(H)–O(H) angle of 121°. However, energy lowering upon relaxation is small: 6 kJ mol^{-1}. We build a two-layer structure, which converges into S4-7, stable, in which the inner atoms approximately reproduce the linear S4-2 structure. Similar linear structures have been studied for uranyl bonding to hydroxide ions.[44,58,59] This additional group is located in the equatorial plane, replacing one or two of the water molecules. $PaO(OH)_2^+$ is isoelectronic to $UO_2(OH)^+$. But the structure of this latter monohydrolysed species is not very well known, for it is highly insoluble. In particular, the coordination number of $UO_2(OH)^+$ is not known in water. We model $PaO(OH)_2^+$ with the inclusion of two explicit solvation layers and apical links. Can we make a reasonable assumption about the coordination number of $PaO(OH)_2^+$? We consider UO_2^{2+} complexes, for which experimental information is available. In water clusters without any coordinating anion, the U–O_{H_2O} distance is close to 242 pm.[60] In ternary uranyl–water–anion clusters, the experimental U–O_{H_2O} distance does not change appreciably: it is 241 pm with inclusion of one to three chloride atoms,[61] 242 pm with one triflate,[62] close to 238 pm with one oxalate,[63] close to 241 pm with one iminodiacetate or 238 pm with one oxydiacetate ions,[64] close to 241 pm with sulfate ions,[65] close to 242 or 240 pm with two nitrate ions,[66,67] close to 238 pm with humic acids,[68] 248 pm being an upper limit observed for the heavily coordinated and strongly anionic complex $UO_2F_4^{2-}$.[69] From these different examples, we conclude that with a single anionic ligand such as OH^-, a typical value for the U–O_{H_2O} bond is 240 pm. With a coordination number of five , in aquo complexes, the calculated average equatorial distance of UO_2^{2+} is 5 pm shorter[25] than its counterpart for $PaOOH^{2+}$, so 245 pm should therefore be a typical value for Pa–O_{H_2O} , With four water molecules in the first coordination sphere (equatorial plane) of $PaO(OH)_2^+$, the calculated Pa–O_{H_2O} average distance lies between 252 and 255 pm in various structures (not shown), whereas with three water molecules it is close to 247 pm (Fig. 4, S4-7). Considering the similarity between $PaOOH^{2+}$ and UO_2^{2+}, and considering the accuracy of distance determination with the method we use,[21,25,70] we suggest that only three water molecules are equatorially coordinated to $PaO(OH)_2^+$ in aqueous solution. As a by-product, other structures, not

presented, indicate the same coordination number for $UO_2(OH)^+$, which is then equal to the gas-phase value.[71] $[UO_2^{2+}(H_2O)_m(OH)_n]^{2-n}$ structures were studied extensively by Ingram *et al.*,[44] and the case $m = 4$, $n = 1$ was studied by Oda *et al.*[59] When the solvent is not modelled, the equatorial uranium–water bond lengths are overestimated, typically by 6 pm.[24,25,72] Considering the calculated published bond-length values, either solvated or in the gas phase with a reduction of 6 pm, we conclude that the computed U–O_w distances in five-coordinated $[UO_2(H_2O)_4(OH)]^{1+}$ significantly overestimate the experimental values.

We find stable structures with two hydration layers (*e.g.* S4-7 in Fig. 4). We can estimate the relative stabilities of the four- and five-coordinated $PaO(OH)_2^+$ species.

$$PaO(OH)_2(H_2O)_4^+(aq) \rightarrow PaO(OH)_2(H_2O)_3^+(aq) + H_2O(l) \quad (1)$$

Upon inclusion of PCM in $PaO(OH)_2^+$/3/6/8 and $PaO(OH)_2^+$/4/8/8 calculations, we find that the five-coordinated species is more stable by 22 kJ mol^{-1}. This difference is within the uncertainties, and we propose that the distance analysis is a more convincing way to asses the coordination number of the predominating species.

$PaO(OH)_2^+$ is commonly identified as the dominating aqueous PaH_{-4}^+ species. Is it the case? We compare its stability relative to PaO_2^+:

$$PaO_2^+(aq) + H_2O(l) \rightarrow PaO(OH)_2^+(aq) \quad (2)$$

We obtain $\Delta_rG_2 = +29$ kJ mol^{-1}, close to $5RT\ln 10$ when reaction (2) is modelled with PaO_2^+/5/10/6 and $PaOOH(OH)^+$/3/6/8. Since PaO_2^+ is unstable, this results suggests that this is also the case for $PaO(OH)_2^+$.

We can estimate the relative stabilities of $PaO(OH)_2^+$ and $PaOOH^{2+}$. The reaction

$$PaO(OH)_2^+(aq) + H^+(aq) \rightarrow PaOOH^{2+}(aq) + H_2O(l) \quad (3)$$

results in $\Delta_rG_3 = -75$ kJ mol^{-1}, corresponding to $\lg K_3 = 13.1$, when modelled with $PaOOH(OH)^+$/3/6/8 and $PaOOH^{2+}$/5/10/6. This negative value indicates that $PaO(OH)_2^+$ would be unstable in aqueous solution at pH below 13.1. Experimental results indicate the half point of the hydrolysis reaction of PaH_{-3}^{2+}, the Pa(v) aqueous dication—hence into PaH_{-4}^+, the aqueous Pa(v) monocation—is $pH_{1/2} = 1.44 \pm 0.71$ ($= -\lg K_2^\circ$ in Table 1). As we will see below $PaOOH^{2+}(aq)$ is the most stable Pa(v) aqueous dication that we calculated in the present study. $PaO(OH)_2^+(aq)$ cannot be the PaH_{-4}^+ mono-cation, since we calculated (see above) that $PaO(OH)_2^+(aq)$ is less stable than $PaO_2^+(aq)$ by 29 kJ mol^{-1}. Now to check whether PaO_2^+ could be PaH_{-4}^+ let us calculate the Gibbs energy of $PaO_2^+(aq)$ protonation by adding the two previous reactions, which results in reaction (7) (see below). We find $\Delta_rG_7 = -45$ kJ mol^{-1}, corresponding to $\lg K = 8.0$, not consistent with the experimental value of 1.44 ± 0.71. These calculated $_rG$ values confirm that Pa(v) monocation is neither $PaO(OH)_2^+$ nor PaO_2^+.

The structures of D_{4h}- and T_d-$Pa(OH)_4^+$

The only remaining PaH_{-4}^+ species are based on $Pa(OH)_4^+$, resulting from the addition of a second water molecule to PaO_2^+. This stoichiometry results in two isomers: a planar structure, with D_{4h} symmetry (S4-4 Fig. 4), and one with T_d symmetry (S4-5 Fig. 4).

We first examine gas-phase D_{4h}-$Pa(OH)_4^+$. Since various linear actinyls are stable in the gas phase (PaO_2^+, $PaOOH^+$, $Pa(OH)_2^{3+}$), it is tempting to consider this structure as a linear actinyl $Pa(OH)_2^{3+}$ to which two equatorial hydroxides are added, but gas-phase in-plane constrained optimization results in an unstable species containing four equivalent hydroxides. Relaxation of this structure in the gas phase results in a stable T_d structure and in an energy decrease of 73 kJ mol^{-1}.

However, we obtained a stable structure by adding two explicit hydration layer to a quasi-D_{4h} symmetry structure, with two water molecules linked to Pa and 17 extra water molecules (the hydroxide and water distances are given in Table 6). We consider the relative stabilities of hydrated PaO_2^+ and D_{4h}-$Pa(OH)_4^+$.

$$PaO_2^+(aq) + 2H_2O(l) \rightarrow Pa(OH)_4^+(aq) \quad (4)$$

For this reaction, modelled with two-layer isomeric complexes including 21 and 19 water molecules, we find $\Delta_rG_4 = +55$ kJ mol^{-1}, which tends to indicate that PaO_2^+ is more stable than the D_{4h} symmetry structure. The instability of this D_{4h} structure is consistent with the instability of planar $PaO(OH)_2^+$. So the D_{4h}-$Pa(OH)_4^+$ is probably not the aqueous monocation of Pa(v). As found in the gas phase, the hydroxide-to-Pa distances are all very similar, so all four hydroxides are equivalent.

In vacuum, the T_d-$Pa(OH)_4^+$ structure is stable, the electronic energy difference with D_{4h}-$Pa(OH)_4^+$ being substantial, as already stated, and larger than Δ_rG_4. This gas-phase energy lowering is an indication that the T_d structure could be the dominating aqueous Pa(v) mono-cation. One would like to compare the relatives stabilities of the two structures or with PaO_2^+. The limited size of our hydration cluster did not allow such comparisons. Few T_d-$Pa(OH)_4^+$ calculations including two hydration layers indicate that water molecules tend to be

Table 6 Typical Pa–ligand distances in aqueous solutions (in pm) and stretching frequencies (ν/cm^{-1}) for linear compounds. Because of splitting, most values are approximate or not available (N.A). Symmetric frequencies are shown but for PaO^{3+} containing structures

Bond	Pa–O (OPaO)	Pa–O (PaO^{3+})	Pa–OH	Pa–H_2O	ν/cm^{-1}
Typical length	190	180	205	245	
PaO_2^+/5/10/6	189	—	—	253	786
$PaO(OH)_2^+$/3/6/8	189	—	211	247	N.A.
$PaOOH^{2+}$/5/10/6	188	—	202	247	N.A.
$Pa(OH)_4^+$/2/4/13	—	—	211	242	N.A.
$Pa(OH)_3^{2+}$/4/8/8	—	—	207	246	N.A.
PaO^{3+}/6/14	—	183	—	241	885
$Pa(OH)_2^{3+}$/5/10/4	—	—	200	241	691
$PaO^{3+}/(SO_4^{2-})_3$	—	185	—	—	830
$PaO^{3+}/(H_2SO_4)_3$	—	177	—	—	980

repelled from the protactinium atom at a distance larger than 260 pm. This water–cation distance has never been observed in actinide or lanthanide solution chemistry, to the best of our knowledge. Other two-layer calculations succeed in keeping water molecules in the vicinity of Pa, increasing the Pa–hydroxide distances. We infer from this that Pa in T_d-$Pa(OH)_4^+$ links directly to water molecules with difficulty, possibly as a result of hydrating coordinated HO^-.

Note that it is known that similar complexes are highly insoluble and precipitate: $An(OH)_4$ for An = Th and U to Pu. For this reason, the impact of hydration on $Pa(OH)_4^+$ stability is still an open question, which should be tackled with quantum dynamics methods. Conversely, the pH predominance domains are broader for these $An(OH)_4(aq)$ species than for the $An(OH)_i^{4-i}(aq)$ ($1 \leq i \leq 3$) less hydrolysed ones:[19] this rather suggests relative stabilization of $An(OH)_4(aq)$.

For the sake of completeness, we compare in the following $AnO_2^{n+}(H_2O)_2$ *vs.* $An(OH)_4^{n+}$ clusters in the gas phase, for Th(IV), Pa(V) and U(VI) (Table 7).

$$AnO_2^{n+}(H_2O)_2 \rightarrow An(OH)_4^{n+} \qquad (5)$$

This is a comparison in the gas phase between isomers and the resulting energies are $\Delta_r G_5$, including thermal and entropy contributions.

It is clear that $Th(OH)_4$ and $UO_2^{2+}(H_2O)_2$ are the more stable in their series, and the difference are so large that solvation cannot reverse the gas-phase stability order. $Pa(OH)_4^+$ is the more stable form in the gas phase.

In T_d-$Pa(OH)_4^+$, the HOMO–LUMO difference is 0.29 a.u., the HOMO−8 to HOMO−9 difference is 0.12 u.a., whereas the HOMO to HOMO−8 energies differ by only 0.04. These three values indicate a 16-electron bonding system. This is confirmed by the NBO analysis, in which each hydroxide is doubly bounded to Protactinium and bears a lone pair.

Conclusion for PaH_{-4}^+ species

PaO_2^+ and $PaO(OH)_2^+$ appear to have comparable stabilities in liquid water, the protonation of these species showing a highly negative free-energy change. Considering experimental results, we infer from this that the dominating PaH_{-4}^+ species is a different hydrolysed form of $PaOOH^{2+}$: among the hydrated PaH_{-4}^+ species we have studied, $Pa(OH)_4^+$ is the only candidate for the dominating aqueous species, assuming that the unusual chemical behaviour of Pa(V)—as compared to the $AnO_2^+(aq)$ species for An ≠ Pa—is caused by the relative instability of $PaH_{-4}^+(aq)$, not specially in an over-stability of PaH_{-5}^0. However, $Pa(OH)_4^+$ detailed interaction with water is still an open question. Isomeric gas-phase reactions indicate that $PaO_2^+(H_2O)_2$ is less stable than $Pa(OH)_4^+$, so for this reaction intermediate between Th(IV) and U(VI).

Table 7 $\Delta_r G_5$ (kJ mol^{-1}) for the isomeric gas phase reactions $AnO_2^{n+}(H_2O)_2/An(OH)_4^{n+}$ (reaction (5)). Gibbs energy reaction for CCSD and CCSD(T) were obtained with the electronic energy and the difference between Gibbs energy and electronic energy from DFT

An	Th	Pa	U
DFT B3LYP	−318	−59	160
CCSD	−328	−23	309
CCSD(T)	−305	−19	247

Dicationic PaH_{-3}^{2+} species

Structures are plotted in Fig. 5.

The structure of $PaOOH^{2+}$

$PaOOH^{2+}$ (S5-1) is the protonated form of PaO_2^+. $PaOOH^{2+}$ is linear (OPaOH), a true minimum in vacuum, with triple bonds in Pa–O and Pa–OH. Like the PaO_2^+ ion, $PaOOH^{2+}$ is isoelectronic with uranyl, and the molecular orbitals are similar, the symmetry of $PaOOH^{2+}$ being lower. The protonation converts a lone pair into an O–H bond, without fundamentally changing the six-bond actinyl structures.

As far as we are aware, $PaOOH^{2+}$ is the only mentioned case of protonation of an actinyl ion in solution. The interaction of the first hydration sphere with $PaOOH^{2+}$ is similar to that described above for PaO_2^+, though the resulting symmetry is C_5. Even though the symmetry of $PaOOH^{2+}$ is lower than that of the uranyl ion, it is clear that the notion of an "equatorial plane", perpendicular to the OPaOH axis, is still valid. To demonstrate this point, we interchanged the OH group with one of the equatorial water molecules in $PaOOH^{2+}/4$. After geometrical relaxation, the resulting species, $(PaO(OH_2))(OH_{eq})(H_2O)_3^{2+}$ was 64 kJ mol^{-1} higher in energy than $PaOOH^{2+}/4$, which contains four equatorial water molecules. The idea of a linear structure including an equatorial plane has been proposed elsewhere.[3]

Straightforward application of our two-sphere methodology to $PaOOH^{2+}$ gives $PaOOH^{2+}/5/10$, but, as already noted for $PaO_2^+/5/10$ above, the resulting structure is not geometrically realistic, so apical links have to be added, as shown in Fig. 5, structure S5-5. The natural charge on O in $PaOOH^{2+}/5/10/6$ is −0.918 e, the PaO and PaO_{OH} distances being 188 and 201 pm, and the H-bond length is 162 pm. The mean equatorial distance $Pa–O_{H_2O}$ is 247 pm, 5 pm longer than in $UO_2^{2+}/5/10/6$.[25] The high negative charge on the apical O in $PaOOH^{2+}$ implies that there is a high tendency for it to form hydrogen bond(s) to (an) H atom(s) of (a) water molecule(s).

The electronic energy of reaction (6)

$$PaO_2^+ + H^+ \rightarrow PaOOH^{2+} \qquad (6)$$

is thermodynamically favourable by a substantial margin in the gas phase (electronic energy change, $\Delta_r E_6 = -267$ kJ mol^{-1} at the B3LYP level with Gaussian 03, and −265 kJ mol^{-1} at the PW91 level with ADF), but this does not correspond to an "intrinsic" stability in aqueous solution. The stability here depends on the H^+ activity, in the same way as aqueous dications are stabilized as compared to aqueous monocations–hence more hydrolysed–in more acidic aqueous solutions. If we include 21 water molecules, protonation is more favourable, as the binding energy of H^+ and PaO_2^+ in two-sphere hydrated structures is close to 800 kJ mol^{-1}. This

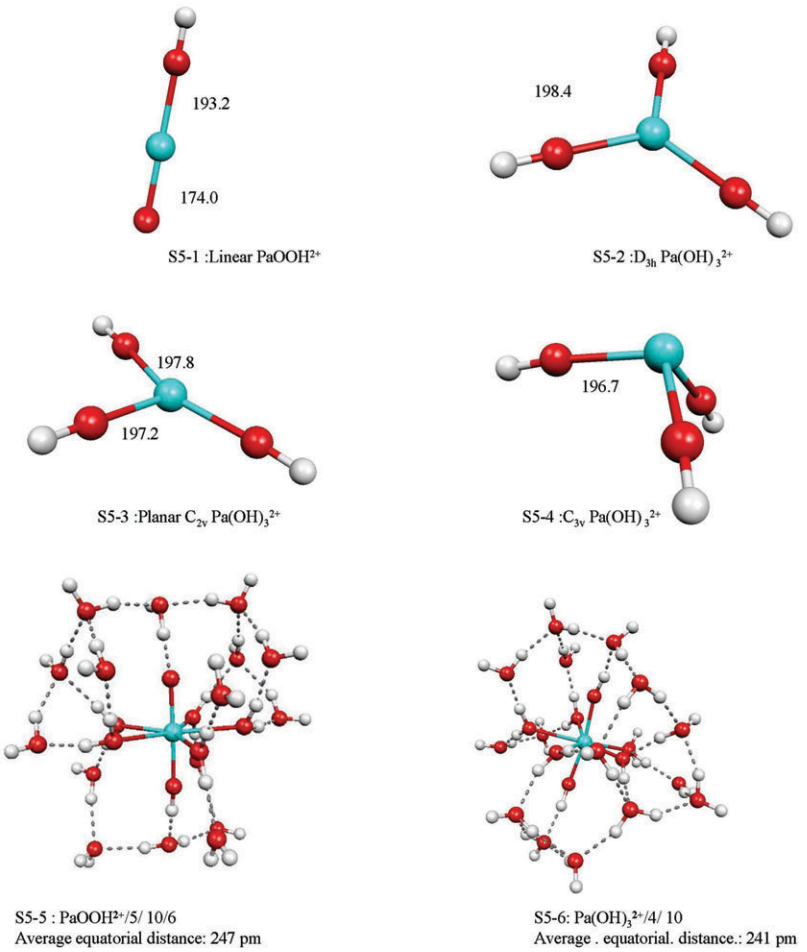

Fig. 5 Protactinium(v) dicationic species in gas phase (S5-1 to 4) and two-layer hydrated (S5-5 and 6). Distances in pm.

reaction can also be modelled with two-sphere clusters embedded in PCM, including H^+ desolvation:

$$PaO_2^+(aq) + H^+(aq) \rightarrow PaOOH^{2+}(aq) \qquad (7)$$

To model reaction (7), we use clusters that both include 21 explicit water molecules. We find $\Delta_r G_7 = -45$ kJ mol^{-1}, close to $-8RT\ln 10$. This indicates that PaO_2^+ is unstable towards protonation up to pH 8.

An intriguing question is the difference in dominating species along the series: $PaOOH^{2+}$, UO_2^+ and NpO_2^+, the latter being very stable. To shed some light on this difference, we consider the reactions

$$PaO_2^+ + UOOH^{2+} \rightarrow PaOOH^{2+} + UO_2^+ \qquad (8)$$

$$PaO_2^+ + NpOOH^{2+} \rightarrow PaOOH^{2+} + NpO_2^+ \qquad (9)$$

In general, it is very difficult to calculate Gibbs energy changes accurately for reactions of actinides in water, but writing these equations makes it much easier. The reason is that these equations are just proton exchanges, so most terms cancel: the reactants and products are so similar that solvation energies, zero point energies and entropy contributions compensate. The result is that the Gibbs energy change is very close to the electronic energy difference in vacuum. We show these two values in Table 5, at two different levels of theory: first with scalar relativity, second with inclusion of spin–orbit coupling. Spin–orbit contributions also compensate almost exactly here, leading to only a trivial difference from the simple scalar relativistic approximation. The Gibbs energy changes for these reactions are strongly negative, since we find -7 and $-10RT\ln 10$, respectively. These results do not prove that PaO_2^+ should protonate or that $NpOOH^{2+}$ should deprotonate. They do show that the known pronounced differences along the series can be interpreted in terms of electronic energies.

The structure of $Pa(OH)_3^{2+}$

In the gas phase, $Pa(OH)_3^{2+}$ can adopt different structures. Optimization results in two planar structures, with D_{3h} (S5-2 Fig. 5) and C_{2v} (S5-3 Fig. 5) symmetries, and a C_{3v} (S5-4 Fig. 5) pyramidal structure. The planar structures are unstable, and the pyramidal structure is a true minimum; the transition from the two former to the latter reduces the electronic energy by 23 kJ mol^{-1}. This reduction is moderate, and we consider the C_{2v} structure for hydration, which results in a stable structure (S5-6) and enables us to study the following reaction:

$$PaOOH^{2+}(aq) + H_2O(l) \rightarrow Pa(OH)_3^{2+}(aq) \qquad (10)$$

We use clusters that include 21 and 20 water molecules, and find $\Delta_r G_{10} = 35$ kJ mol^{-1}. This indicates that linear $PaOOH^{2+}$ is the more stable species, despite the existence of a C_{3v}-$Pa(OH)_3^{2+}$ which is more stable in the gas phase than the C_{2v} we use for starting optimisation of two-layer solvation.

Conclusion for PaH_{-3}^{2+} species

$PaOOH^{2+}$ appears to be the stable species in the PaH_{-3}^{2+} series.

Tricationic PaH_{-2}^{3+} species

There are two tricationic species, plotted in Fig. 6, S6-1 and S6-2.

The structure of $Pa(OH)_2^{3+}$

Experimental studies indicate that a trication cannot be ruled out in very acidic ($[H^+] > 1$ mol L^{-1}) aqueous solutions.[17] This species has been written PaO^{3+} and has been studied by quantum calculations.[3] However, protonation of the above stable $PaOOH^{2+}$ dication produces linear $Pa(OH)_2^{3+}$, which is isoelectronic to PaO_2^+ and $PaOOH^{2+}$. As in single protonation, a lone pair is converted into an O–H bond, without substantially changing the six-bond actinyl structure. Upon addition of two hydration layers and apical links, we find a five-coordinated structure whose actinyl bond length is 200.8 pm and with an average equatorial distance of 240.7 pm (S6-4 in Fig. 6).

Diprotonation of PaO_2^+

Using a PaO_2^+ two-sphere model in which we protonate apical water molecules—linked to O_{yl}–resulting in H_3O^+ in apical positions, we find that the two apical protons link to the O_{yl}, and that this diprotonation does not show any activation barrier. The addition of a second H^+ to $PaOOH^{2+}$, to give $Pa(OH)_2^{3+}$, a linear species that is a true minimum, is unfavourable in vacuum by 300 kJ mol^{-1}. These gas-phase considerations do not include H^+ desolvation, so we now include the solvent. Protons in aqueous solution experience the competitive attraction from the O_{yl} and from the solvent: could this account for PaO_2^+ unstability? We estimate for this the Gibbs energy of the following reaction:

$$PaO_2^+(aq) + 2H^+(aq) \rightarrow Pa(OH)_2^{3+}(aq) \qquad (11)$$

Both structures have been detailed previously. The Gibbs energy of this reaction is evaluated using two-layer hydrated structures including 21 and 19 water molecules, respectively. We find $\Delta_r G_{11} = -55$ kJ mol^{-1}, close to $10RT$. This corresponds to an equivalence point at pH 5. It is established that Pa(v)-trications do not appear at such high pH, for they are doubly-hydrolysed into a monocationic species. This result is a theoretical confirmation of PaO_2^+ instability. It corroborates the hypothesis that PaO_2^+ is not the dominating monocation of Pa(v), but that it is a hydrolysed form of $Pa(OH)_2^{3+}$. It is noteworthy that axial protonation and radial hydrolysis are synergistic, and not antagonist. In the gas phase, the Pa(v) NPA charge increases from 2.48 *e* in PaO_2^+ to 3.31 *e* in $Pa(OH)_2^{3+}$. This increases the hydrolysis constant by 9 units,[9] indicating that the reaction path from PaO_2^+ to $Pa(OH)_4^+$ could be modelled dynamically with successive protonations and hydrolyses.

Proton exchange energy values in Table 5, along with Gibbs energy for reaction (11), confirm that neither UO_2^+ nor NpO_2^+ protonate.

The structure of PaO^{3+}

We made some trial calculations on the Pa(v)/SO_4^{2-}/H^+/H_2O system, to compare the shortest Pa–O distance consistent with

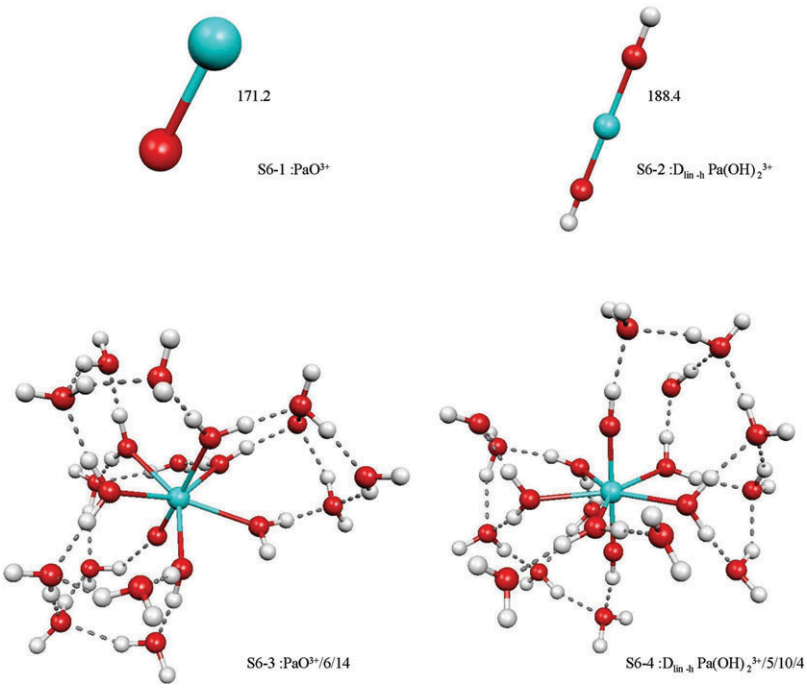

Fig. 6 Protactinium(v) tricationic species, in gas phase (S6-1 and 2) and two-layer hydrated (S6-3 and 4). Distances in pm.

recent EXAFS measurements. As mentioned above, it is not easy to interpret the available data in sulfate solution. EXAFS data have been interpreted with five SO_4^{2-} coordinated to Pa,[17] although, to our knowledge, coordination of five sulfates on a trication has never been observed. Indeed, an upper limit of three SO_4^{2-} on Pa(v) was proposed later.[73] The EXAFS distance has been reported to be 172 pm,[17] whereas we calculated 200 pm for $Pa(OH)_2^{3+}$(aq) as modelled by $Pa(OH)_2^{3+}$/5/10/4 This value substantially overestimates the experimental result. We infer that the $Pa(OH)_2^{3+}$ unit was not part of the major aqueous Pa(v) sulfate complex. The smallest Pa–O EXAFS distance should indeed be attributed to the formation of the PaO^{3+} cation in the complex.

We performed many calculations on PaO^{3+} coordinated with sulfate, mono- and dihydrogenosulfate. We did not succeed in reproducing the experimental Pa–O distance associated with the claimed coordination of five sulfates: (three monodentate and two bidentate giving a coordination of seven).[17] We suppose that the size of sulfate groups and the strongly Pa-bonded oxygen are inhibitory hindrances to this high coordination number. When the inclusion of solvent molecules, either water or sulfates, approaches the coordination numbers five or six, we find Pa=O distances close to 180 pm (Table 6). 13 M H_2SO_4 can hardly be considered as an aqueous solution, the solute and solvent concentration being comparable. This concentration is a major hindrance to acid dissociation. We present two limiting complexes in Fig. 7, S7-1 and S7-2, fully dissociated and fully undissociated triligand complexes, for three (dihydro-) sulfate, the established coordination number. The inclusion of dihydrogenosulfate is not intended to be realistic, but only aims at calculating a limiting complex. Similarly, the inclusion of an extra water molecule among the ligands is not excluded, but it would have little impact on the parameter under concern, which is the Pa–O bond length. The difference from the smallest experimental distance is larger than the commonly observed accuracy of the method we use, 1%, either in this paper for PaF_7^{2-}, or for uranyl[25] or neptunyl,[74] to cite a few. We note that in the Fig. 4 of the quoted reference, the fitted modulus of the Fourier transform underestimates the PaO $R + \Phi$ peak by 5–10 pm. Indeed, by adding 7 pm to the proposed value, we find a typical calculated value for the Pa–O distance in a six-coordinated complex.

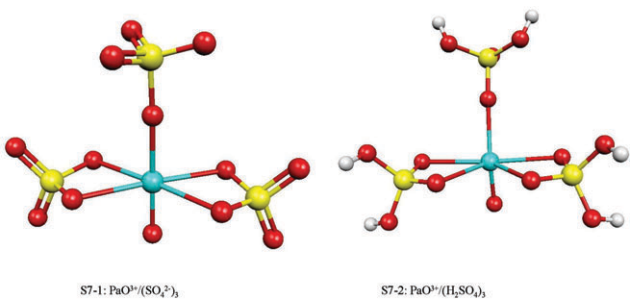

Fig. 7 Hypothetical limiting PaO^{3+}/3 ligand complexes for Pa(v) in sulfate solution, including mono- and bidentate ligands. See text for comments.

What structure could an aquo PaO^{3+} cluster adopt? We model a cluster which includes six water molecules in the first shell and 14 in the second shell (structure S6-3 in Fig. 6). This results in an average water distance of 241 pm, whereas the inclusion of seven waters results in a distance of 246 pm. Considering that this distance is 249 for NpO_2^+ or 242 pm for UO_2^{2+}, our calculations suggest that the PaO^{3+} cannot be seven-coordinated, six being an upper limit. The coordination number of six is also consistent with the $PaO(SO_4)_3^-$ limiting complex proposed in the literature[73] and with one-layer models.[3]

The PaO^{3+} geometry is certainly confirmed in the aqueous sulfate (or hydrogenosulfate) complex, but this does not necessarily mean that PaO^{3+}(aq) is also more stable than $Pa(OH)_2^{3+}$(aq) in non-complexing very concentrated acidic media. $Pa(OH)_2^{3+}$ can be considered as an isomer of PaO^{3+} in liquid water. What is the value of the $[Pa(OH)_2^{3+}(aq)]/[PaO^{3+}(aq)]$ ratio? Is it better to write $Pa(OH)_2^{3+}$(aq) instead of PaO^{3+}(aq), the only notation proposed in the literature? This ratio originates from the Gibbs' energy change for the following reaction:

$$PaO^{3+}(aq) + H_2O(l) \rightarrow Pa(OH)_2^{3+}(aq) \qquad (12)$$

We model this reaction with isomeric clusters, which include 20 and 19 water molecules, respectively. With this PaO^{3+} six-coordinated cluster and a $Pa(OH)_2^{3+}$/5/10/4, we find $\Delta_r G_{12} = -6$ kJ mol^{-1}. This value is too small for us to discard any of the structures. The $Pa(OH)_2^{3+}$ ion could exist in non-sulfate solutions. To our knowledge, this possibility has never been examined.

Conclusion for PaH_{-2}^{3+}

Although PaO^{3+} is confirmed in concentrated sulfate solution, $Pa(OH)_2^{3+}$ cannot be disregarded in non-complexing media at pH less than 0. The structure of this $Pa(OH)_2^{3+}$ species is readily obtained by diprotonation of PaO_2^+.

Typical distances

Chemical bonds have characteristic lengths. From all the structural results we obtained, we can state the following results: any observed distance in protactinium aqueous solution can be related to a particular bond length, shown in Table 6. The observed variations within our structures are typically less than 5 pm.

We note that the Pa–O_{oxide} distances are smaller than the Pa–OH ones. The Pa–O_{oxide} distance is smaller for PaO^{3+} than in linear protactinyl (PaO_2^+) and its protonated forms (Pa–O_{oxide} in $Pa(OH)_2^{3+}$ and $PaOOH^{2+}$). The Pa–OH distances are smaller in linear $Pa(OH)_2^{3+}$ and $PaOOH^{2+}$ than in bent or equatorial $PaO(OH)_2^+$, and $Pa(OH)_4^+$ structures. These distances are also correlated to the total charges of the molecular ions: the Pa–O distances decrease with the total formal charge. The differences between these values should enable us to discriminate them by EXAFS, and also from many other ligands, such as chloride.

Conclusions

We have used DFT calculations to study the structures of several protactinium-containing species. The accuracy of our computational methods for calculating metal–ligand distances has already been established for the uranyl ion: here it is confirmed for PaF_7^{2-}(aq) and PaO^{3+}(aq).

PaO_2^{+} is linear, similar to higher actinyls, but its stability is controversial in aqueous solution. Explicit models show that this potential instability may be attributed to the highly negative charge on the oxygen atoms, which is confirmed by comparison with the stable AnO_2^{+} species of heavier actinides(v). Comparison along the isolectronic series ThO_2, PaO_2^{+} and UO_2^{2+} confirms the increasing importance along the series of f functions, and of their role in the linearity of O–An–O. The protonation of PaO_2^{+} is energetically favoured in comparison with UO_2^{+} and NpO_2^{+}. We suggest that the known and paradoxical stabilities of both the complexes $PaOOH^{2+}$(aq) and NpO_2^{+}(aq) can thus be explained by this substantial electronic difference between Pa and Np. PaO_2^{+} shows instability towards mono- and diprotonations. The diprotonation of PaO_2^{+}(aq) species to give $Pa(OH)_2^{3+}$(aq) is favoured at a pH value which implies double-hydrolysis of this highly charged species. The high Gibbs energy variation for this diprotonation confirms PaO_2^{+} instability. $PaO(OH)_2^{+}$(aq) shows similar stability to PaO_2^{+}(aq), D_{4h}-$Pa(OH)_4^{+}$(aq) being less stable. These species can not account for the existence of a pH stability domain for the monocation PaH_{-4}^{+} This indicates the existence of a different stable PaH_{-4}^{+}(aq) species, the only remaining one being T_d-$Pa(OH)_4^{+}$(aq): we indeed find it is more stable than D_{4h}-$Pa(OH)_4^{+}$ in the gas phase, but their detailed solvation is still an open question.

There are fewer PaH_{-3}^{2+} species. $PaOOH^{2+}$ results from the protonation of PaO_2^{+}. The electronic structure of $PaOOH_2^{+}$ is similar to that of the uranyl ion. Note that this species is the only known protonated actinide in solution. We propose a structure for this cation in water. $PaOOH^{2+}$(aq) is very stable. $Pa(OH)_3^{2+}$(aq) species is less stable.

There are two PaH_{-2}^{3+} species. Our calculations unambiguously confirmed the stability of PaO^{3+}(aq) inside a complex formed in concentrated sulfate aqueous solutions. However, in other conditions, the existence of $Pa(OH)_2^{3+}$(aq) cannot be precluded since the free-energy difference is insignificant.

The case of protactinium in aqueous fluoride-containing solutions illustrates nicely the complementarity between experimental and theoretical structure determinations. We have reduced the number of possible structures in hydrofluoric media, and shown that a coordination number of seven is the only one that gives a calculated Pa–F distance consistent with the experimental EXAFS value. This result is interesting and useful, since EXAFS does not yield very precise data for coordination numbers or for atom discrimination. One usually uses theoretical chemistry to determine coordination numbers from the energetic point of view, which is fundamentally right. However, we believe that the structural—or steric—point of view is a much more efficient speciation tool in the particular case of ions in aqueous solution.

With DFT, we could include many solvent molecules, whose presence in the model is decisive. However, the various protonations or hydroxidations encountered, *e.g.* of PaO_2^{+}, result from protactinium's electronic properties which remain to be tackled in smaller clusters with high-level modelling.

The protonation of PaO_2^{+}(aq) increases its susceptibility to hydrolysis: this result is a precious indication for the dynamic modelling of reaction paths from PaO_2^{+}(aq) to $Pa(OH)_4^{+}$(aq).

References

1 M. Straka, K. G. Dyall and P. Pyykkö, *Theor. Chem. Acc.*, 2001, **106**, 393.
2 J. K. Gibson and R. G. Haire, *Inorg. Chem.*, 2002, **41**, 5897.
3 T. Toraishi, T. Tsuneda and S. Tanaka, *J. Phys. Chem. A*, 2006, **110**, 13303.
4 O. L. Keller, Jr, *Inorg. Chem.*, 1963, **2**, 783.
5 D. Trubert, C. Le Naour, C. Jaussaud and O. Mrad, *J. Solution Chem.*, 2003, **32**, 505.
6 K. G. Dyall, *Mol. Phys.*, 1999, **96**, 511.
7 P. Pyykkö, L. J. Laakkonen and K. Tatsumi, *Inorg. Chem.*, 1989, **28**, 1801–1805.
8 K. Tatsumi and R. Hoffman, *Inorg. Chem.*, 1980, **19**, 2656–2658.
9 P. Vitorge, V. Phrommavanh, B. Siboulet, D. You, T. Vercouter, M. Descostes, C. J. Marsden, C. Beaucaire and J. P. Gaudet, *C. R. Acad. Sci., Ser. IIb: Chim*, 2007, **10**(10–11), 978–993.
10 M. Straka, P. Hrobarik and M. Kaupp, *J. Am. Chem. Soc.*, 2005, **127**, 2591.
11 V. Pershina and T. Bastug, *Radiochim. Acta*, 1999, **84**, 79.
12 N. Kaltsoyannis and B. E. Bursten, *Inorg. Chem.*, 1995, **34**, 2735.
13 B. Siboulet, P. Vitorge and C. J. Marsden, GdR PARIS, 16–17 mars 2006, Avignon (France), http://www-ist.cea.fr/publicea/exl-doc/200600002864_s1.pdf, see also 3rd Conference on Very Heavy Metals (VHM–2006) 07-12/03/2006, Aubrac (France), http://www-ist.cea.fr/publicea/exl-doc/200600002604_s1.pdf.
14 R. L. Martin, P. J. Hay and L. R. Pratt, *J. Phys. Chem. A*, 1998, **102**, 3565.
15 D. Trubert, C. Le Naour and C. Jaussaud, *J. Solution Chem.*, 2002, **31**, 261.
16 R. Muxart and R. Guillaumont, *Protactinium*, Masson et Cie, Paris, France, 1974.
17 C. Le Naour, D. Trubert, M. V. Di Giandomenico, C. Fillaux, C. Den Auwer, P. Moisy and C. Hennig, *Inorg. Chem.*, 2005, **44**, 9542.
18 R. Guillaumont, Université de Paris, 1966.
19 R. Lemire, J. Fuger, H. Nitsche, M. Rand, K. Spahiu, J. Sullivan, W. Ullman and P. Vitorge, *Chemical Thermodynamics of Neptunium an Plutonium*, /NEA OECD Elsevier, Amsterdam, 2001.
20 P. Vitorge and H. Capdevila, *Radiochim. Acta*, 2003, **91**, 623–631.
21 G. A. Shamov and G. Schreckenbach, *J. Phys. Chem. A*, 2005, **109**, 10961.
22 B. Fourest, J. Perrone, P. Tarapcik and E. Giffaut, *J. Solution Chem.*, 2004, **33**, 957.
23 C. Le Naour, D. Trubert and C. Jaussaud, *J. Solution Chem.*, 2003, **32**, 489.
24 K. E. Gutowski and D. A. Dixon, *J. Phys. Chem. A*, 2006, **110**, 8840.
25 B. Siboulet, C. J. Marsden and P. Vitorge, *Chem. Phys.*, 2006, **326**, 289.
26 A. D. Becke, *J. Chem. Phys.*, 1993, **98**, 5468.
27 M. J. Frisch, G. W. Trucks, H. B. Schlegel, G. E. Scuseria, M. A. Robb, J. R. Cheeseman, J. A. Montgomery, Jr., T. Vreven, K. N. Kudin, J. C. Burant, J. M. Millam, S. S. Iyengar, J. Tomasi, V. Barone, B. Mennucci, M. Cossi, G. Scalmani, N. Rega, G. A. Petersson, H. Nakatsuji, M. Hada, M. Ehara, K. Toyota, R. Fukuda, J. Hasegawa, M. Ishida, T. Nakajima, Y. Honda, O. Kitao, H. Nakai, M. Klene, X. Li, J. E. Knox, H. P. Hratchian, J. B. Cross, V. Bakken, C. Adamo, J. Jaramillo, R. Gomperts, R. E. Stratmann, O. Yazyev, A. J. Austin, R. Cammi, C. Pomelli, J. Ochterski, P. Y. Ayala, K. Morokuma, G. A. Voth, P. Salvador, J. J. Dannenberg, V. G. Zakrzewski, S. Dapprich, A. D. Daniels, M. C. Strain, O. Farkas, D. K. Malick, A. D. Rabuck, K. Raghavachari, J. B. Foresman, J. V. Ortiz, Q. Cui, A. G. Baboul, S. Clifford, J. Cioslowski, B. B. Stefanov, G. Liu, A. Liashenko, P. Piskorz,

I. Komaromi, R. L. Martin, D. J. Fox, T. Keith, M. A. Al-Laham, C. Y. Peng, A. Nanayakkara, M. Challacombe, P. M. W. Gill, B. G. Johnson, W. Chen, M. W. Wong, C. Gonzalez and J. A. Pople, *GAUSSIAN 03 (Revision B.02)*, Gaussian, Inc., Wallingford, CT, 2004.
28 A. E. Reed, L. A. Curtiss, F. Weinhold and W. Aas, *Chem. Rev.*, 1988, **88**, 899.
29 E. D. Glendening, A. E. Reed, J. E. Carpenter and F. Weinhold, *NBO Version 3.1*, 1998.
30 A. E. Clark, J. L. Sonnenberg, P. J. Hay and R. L. Martin, *J. Chem. Phys.*, 2004, **121**, 2563.
31 W. Küchle, M. Dolg, H. Stoll and H. Preuss, *J. Chem. Phys.*, 1994, **100**, 7535.
32 N. Ismail, J. L. Heully, T. Saue, J. P. Daudey and C. J. Marsden, *Chem. Phys. Lett.*, 1999, **300**, 296.
33 Y. Bouteiller, C. Mijoule, M. Nizam, J. C. Barthelat, J. P. Daudey and M. Pelissier, *Mol. Phys.*, 1988, **65**, 295.
34 T. H. Dunning and P. J. Hay, *Modern Theoretical Chemistry 3*, ed. H. F. Schaefer, Plenum, New York, 1977.
35 T. H. Dunning, *J. Chem. Phys.*, 1971, **55**, 716.
36 R. B. J. S. Krishnan, R. Seeger and J. A. Pople, *J. Chem. Phys.*, 1980, **72**, 650.
37 ADF 2006: E. J. Baerends, J. Autschbach, A. Bérces, F. M. Bickelhaupt, C. Bo, P. M. Boerrigter, L. Cavallo, D. P. Chong, L. Deng, R. M. Dickson, D. E. Ellis, M. van Faassen, L. Fan, T. H. Fischer, C. Fonseca Guerra, S. J. A. van Gisbergen, J. A. Groeneveld, O. V. Gritsenko, M. Grüning, F. E. Harris, P. van den Hoeck, C. R. Jacob, H. Jacobsen, L. Jensen, G. van Kessel, F. Koostra, E. van Lenthe, D. A. McCormack, A. Michalak, J. Neugebauer, V. P. Osinga, S. Patchkovskii, P. H. T. Philipsen, D. Post, C. C. Pye, W. Ravenek, P. Ros, P. R. T. Schipper, G. Schreckenbach, J. G. Snijders, M. Solà, M. Swart, D. Swerhone, G. te Velde, P. Vernooijs, L. Versluis, L. Visscher, O. Visser, F. Wang, T. A. Weselowski, E. van Wezenbeek, G. Wiesenekker, S. K. Wolff, T. K. Woo, A. L. Yakovlev and T. Ziegler.
38 C. Fonseca Guerra, J. G. Snijders, G. te Velde and E. J. Baerends, *Theor. Chem. Acc.*, 1998, **99**, 931.
39 G. te Velde, F. M. Bickelhaupt, S. J. A. van Gisbergen, C. Fonseca Guerra, E. J. Baerends, J. G. Snijders and T. Ziegler, *J. Comput. Chem.*, 2001, **22**, 931.
40 I. Grenthe, J. Fuger, J. M. Konings, R. Lemire, A. B. Muller, C. Nguyen-Trung and H. Wanner, *Chemical Thermodynamics of Uranium*, ed. H. Wanner and I. Forest, OECD NEA, Data Bank, Issy-les-moulineaux, 2004.
41 C. G. Zhan and D. A. Dixon, *J. Phys. Chem. A*, 2001, **105**, 11534.
42 C. G. Zhan and D. A. Dixon, *J. Phys. Chem. A*, 2002, **106**, 9737.
43 I. Infante and L. Visscher, *J. Chem. Phys.*, 2004, **121**, 5783.
44 K. I. M. Ingram, L. J. L. Haller and N. Kaltsoyannis, *Dalton Trans.*, 2006, 2403.
45 P. Guilbaud and G. Wipff, *J. Mol. Struct. (THEOCHEM)*, 1996, **366**, 55.
46 M. Bühl, R. Diss and G. Wipff, *J. Am. Chem. Soc.*, 2005, **127**, 13506.
47 D. Brown and A. G. Maddock, *Q. Rev. Chem. Soc.*, 1963, 289.
48 T. Yamaguchi, M. Nomura, H. Wakita and H. Ohtaki, *J. Chem. Phys.*, 1988, **89**, 5153.
49 H. Moll, M. A. Denecke, F. Jalilehvand, M. Sandstrom and I. Grenthe, *Inorg. Chem.*, 1999, **38**, 1795.
50 V. Vallet, U. Wahlgren, B. Schimmelpfennig, H. Moll, Z. Szabo and I. Grenthe, *Inorg. Chem.*, 2001, **40**, 3516.
51 P. Flükiger, H. P. Lüthi, S. Portmann and S. J. Weber, *Swiss Center for Scientific Computing*, Manno, Switzerland, 2002.
52 S. Portmann and H. P. Lüthi, *Chimia*, 2000, **54**, 766.
53 P. J. Hay, R. L. Martin and G. Schreckenbach, *J. Phys. Chem. A*, 2000, **104**, 6259.
54 I. Infante and L. Visscher, 2007, unpublished work.
55 I. Infante, A. S. P. Gomes and L. Visscher, *J. Chem. Phys.*, 2006, **125**, 74301.
56 C. Den Auwer, P. Guilbaud, D. Guillaumont, P. Moisy, M. V. Di Giandomenico, C. Le Naour, D. Trubert, E. Simoni, C. Hennig, A. C. Scheinost and S. Conradson, *AIP Conf. Proc.*, 2007, **882**, 184–186.
57 S. D. Conradson, *Appl. Spectrosc.*, 1998, **52**, 252A.
58 T. Privalov, B. Schimmelpfennig, U. Wahlgren and I. Grenthe, *J. Phys. Chem. A*, 2002, **106**, 11277.
59 Y. Oda and A. Aoshima, *J. Nucl. Sci. Technol.*, 2002, **39**, 647.
60 J. Neuefeind, L. Soderholm and S. Skanthakumar, *J. Phys. Chem. A*, 2004, **108**, 2733.
61 C. Hennig, J. Tutschku, A. Rossberg, G. Bernhard and A. C. Scheinost, *Inorg. Chem.*, 2005, **44**, 6655.
62 L. Semon, C. Boehme, I. Billard, C. Hennig, K. Lutzenkirchen, T. Reich, A. Rossberg, I. Rossini and G. Wipff, *ChemPhysChem*, 2001, **2**, 591.
63 V. Vallet, H. Moll, U. Wahlgren, Z. Szabo and I. Grenthe, *Inorg. Chem.*, 2003, **42**, 1982.
64 J. Jiang, J. C. Renshaw, M. J. Sarsfield, F. R. Livens, D. Collison, J. M. Charnock and H. Eccles, *Inorg. Chem.*, 2003, **42**, 1233.
65 H. Moll, T. Reich, C. Hennig, A. Rossberg, Z. Szabo and I. Grenthe, *Radiochim. Acta*, 2000, **88**, 559.
66 H. A. Thompson, G. E. Brown and G. A. Parks, *Am. Mineral.*, 1997, **82**, 483.
67 T. Yaita, H. Narita, S. Suzuki, S. Tachimori, H. Shiwaku and H. Motohashi, *J. Alloys Compd.*, 1998, **271**, 184.
68 M. A. Denecke, T. Reich, M. Bubner, S. Pompe, K. H. Heise, H. Nitsche, P. G. Allen, J. J. Bucher, N. M. Edelstein and D. K. Shuh, *J. Alloys Compd.*, 1998, **271**, 123.
69 V. Vallet, U. Wahlgren, B. Schimmelpfennig, Z. Szabo and I. Grenthe, *J. Am. Chem. Soc.*, 2001, **123**, 11999.
70 M. Bühl and V. Golubnychiy, *Inorg. Chem.*, 2007, **46**, 8129–8131.
71 G. L. Gresham, A. K. Gianotto, P. D. Harrington, L. B. Cao, J. R. Scott, J. E. Olson, A. D. Appelhans, M. J. Van Stipdonk and G. S. Groenewold, *J. Phys. Chem. A*, 2003, **107**, 8530.
72 L. Gagliardi, I. Grenthe and B. O. Roos, *Inorg. Chem.*, 2001, **40**, 2976.
73 M. V. T. Di Giandomenico and D. Le Naour, C, *Radiochim. Acta*, 2007, **95**, 617–623.
74 H. Bolvin, U. Wahlgren, H. Moll, T. Reich, G. Geipel, T. Fanghanel and I. Grenthe, *J. Phys. Chem. A*, 2001, **105**, 11441.

